Two-Phase LLC Converter using a Flying Capacitor for High Output Current Applications

Or Kirshenboim, *Student Member, IEEE*, and Mor Mordechai Peretz, *Member, IEEE*

The Center for Power Electronics and Mixed-Signal IC
Department of Electrical and Computer Engineering
Ben-Gurion University of the Negev
P.O. Box 653, Beer-Sheva, 8410501 Israel
orkir@post.bgu.ac.il morp@ee.bgu.ac.il
http://www.ee.bgu.ac.il/~pemic

***Abstract*- This paper introduces a new two-phase interleaved flying-capacitor LLC converter topology with high output current applications. Compared to a conventional two-phase LLC converter, the new converter adds a single capacitor that contributes to lower voltage stress on the primary side's switches, automatically balances the current distribution between the phases and enhances the power processing capabilities. All the attractive features of LLC converters are preserved, such as zero-voltage switching on the primary side's MOSFETs, zero-current switching on the secondary side's power devices, narrow switching frequency range and simple design. Full principle of operation and analysis of the converter is described, as well as the converter's primary characteristics and the impact of non-ideal components on the current sharing behavior.**

***Index terms*- DC-DC converters, resonant converters, current sharing.**

I. INTRODUCTION

TODAY'S power converters are required to deliver more power and achieve high efficiency over a wide load range. The LLC resonant converter topology is able to address such challenges and is advantageous in front-end DC-DC conversion applications as a result of the zero-voltage switching (ZVS) for the primary side's MOSFETs and zero-current switching (ZCS) for the secondary side's power devices [1]-[5]. In addition, it features narrow switching frequency range to facilitate regulation, fast transient response and relatively low cost mainly due to incorporation of the transformer's leakage inductance as the resonant inductor. In particular in its half-bridge implementation, the topology has been widely and successfully applied to flat panel TVs, 80+ ATX and small form factor PCs, where the requirements on efficiency, power density and EMC compliance of their switching mode power supplies (SMPS) are getting more and more stringent.

In high power applications where the current stress in a converter becomes high, paralleling of two (or more) converters, namely multi-phase operation, is a good solution for distribution of the current stress and it has been broadly investigated for both PWM [6]-[10] and resonant converters [11]-[13]. It has been found that multi-phase operation of LLC converters introduces implementation challenges that are typically related to the load current sharing between the converter's phases [11]-[24]. Current sharing is required to increase the power processing capability, maintain high efficiency and improve the reliability since the thermal stress is better distributed. Therefore, current sharing is considered mandatory in multi-phase LLC converters operation.

The main reason for an unbalanced load sharing between converter's phases lays in the difference between the components of the resonant networks. When interleaving phases, since the operation hinges on equivalent switching frequency of the different phases, mismatches in the resonant tank components impact the current distribution between the phases [13]. This is since only one phase operates at the frequency where the required voltage gain is achieved. Even small differences, within the resonant components values' tolerances, can have a severe effect on the current sharing and one phase will deliver most of the load current when other phases deliver a significantly smaller portion of it [19]. Several solutions have been proposed to achieve current sharing [12]-[24]. These solutions are used to match the resonant tanks components' values and can be classified as active or passive. In the active solutions, additional circuitry is added in order to control the resonant tank capacitance [13], [14] or inductance [15], to control the switching frequency [16] or to control the phase shift between the phases in case of three-phase structure [17]. However, these solutions suffer from complex control and implementation issues, high component count and high cost. The passive solutions use a common capacitor [18] or common inductor [19], [20] for impedance matching of the phases [21]. Another passive solution that achieves good current sharing is based on series-input connected capacitors [22], [23].

To further improve the power processing capability of LLC resonant converters, multi-level operation has been investigated [25]. This approach provides lower voltage stress on the primary side's power devices and allows for the use of lower voltage rated MOSFETs with lower $R_{DS(on)}$ per silicon area. The use of lower voltage rated MOSFETs reduces the conduction losses for a given area while maintaining very low

switching losses due to ZVS. Another important feature of the multi-level operation is that the required dead-time and magnetizing inductance current to achieve ZVS can be decreased since lower energy is stored in the parasitic capacitances of the MOSFETs, which further improves the efficiency of the converter.

The objective of this study is to introduce a new two-phase interleaved flying-capacitor LLC (TIFLLC) resonant converter topology that combines multi-phase and multi-level operations. The new topology, shown in Fig. 1, incorporates a flying-capacitor that lowers the voltage stress on the primary side's MOSFETs, balances the current delivered by the two phases and enhances the power processing characteristics. A significant advantage of the TIFLLC converter topology is that it preserves the benefits of conventional LLC converters such as soft-switching on all power devices, wide load range, narrow switching frequency range as well as excels with high efficiency. These advantages make the topology an attractive candidate for high output current applications.

The rest of the paper is organized as follows: Section II presents the TIFLLC converter topology principle of operation and provides typical key waveforms of the new converter. Design considerations and details of the flying-capacitor are provided in Section III. Next, the current sharing and enhanced power processing characteristics are described in Section IV. Experimental results are provided in Section V. Section VI concludes the paper.

II. Principle of Operation

The TIFLLC converter, shown in Fig. 1, combines the benefits of a switched-capacitor circuit and a series-resonant LLC converter. This topology adds a single capacitor C_t to the component count of a conventional two-phase LLC converter. The converter's configuration and waveforms resemble the ones of the two-phase interleaved LLC converter, with the benefits of lower voltage stress transistors.

The operation of the TIFLLC converter is similar to the one of a conventional two-phase interleaved LLC converter with 180^0 phase delay, i.e., when the switching node (SW_a/SW_b) of one phase is high, then the switching node of the other phase is low. Therefore, two switching states are recognized as shown in Fig. 2 with the corresponding waveforms (obtained by a PSIM simulation) shown in Fig. 3: State I: phase *a* is on and phase *b* is off; State II: phase *a* is off and phase *b* is on.

In state I, depicted in Fig. 2(a), switches Q_{1a} and Q_{2b} are on, the input voltage connects to phase *a* through the flying-capacitor C_t and the applied voltage on its resonant tank is V_{in}-V_{Ct}, while the resonant tank of phase *b* connects to ground via Q_{2b}. At the secondary side, switches S_{2a} and S_{1b} are on for synchronous rectification operation. State II is shown in Fig. 2(b). Here, switches Q_{1b} and Q_{2a} are on and the flying-capacitor acts as the source for phase *b*, imposing a voltage of V_{Ct} on its resonant tank, while the resonant tank of phase *a* connects to ground; switches S_{1a} and S_{2b} are on for synchronous rectification of the output current. As in conventional LLC resonant

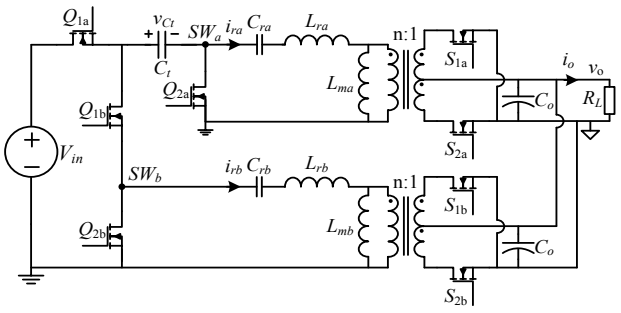

Fig. 1. Two-phase interleaved flying-capacitor LLC (TIFLLC) converter topology.

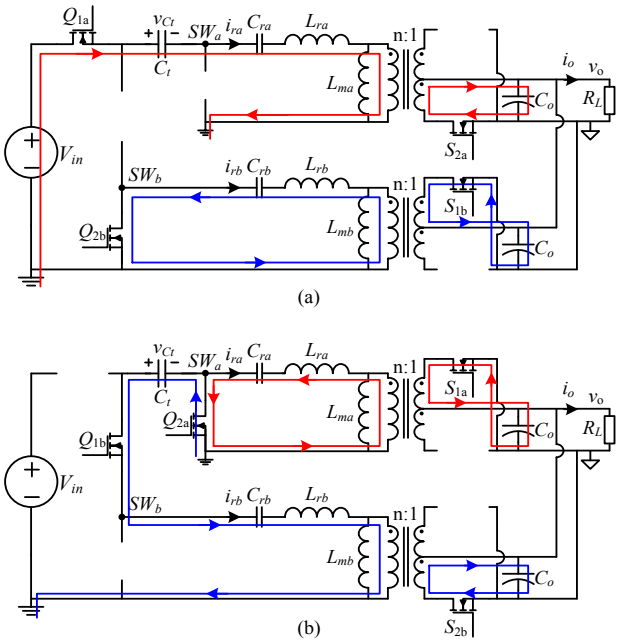

Fig. 2. Current paths in the TIFLLC converter: (a) State I: phase *a* is on and phase *b* is off, (b) State II: phase *a* is off and phase *b* is on.

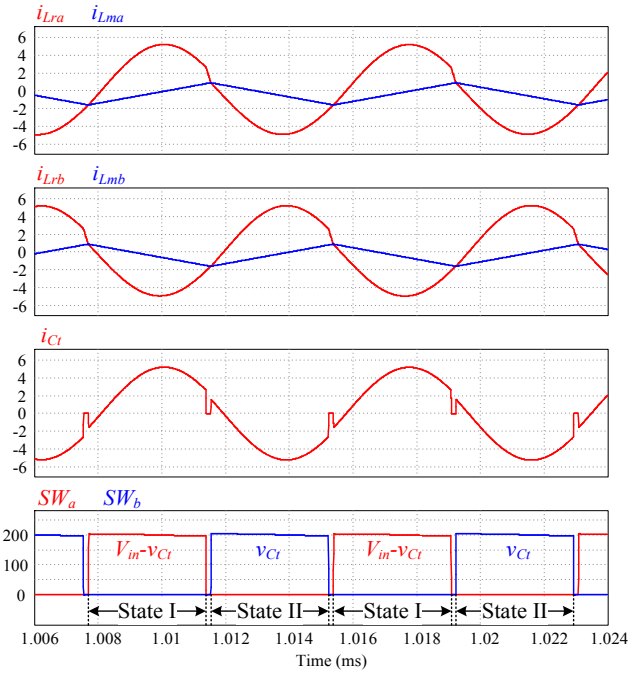

Fig. 3. Typical waveforms of the TIFLLC converter.

converters, dead-time between the two switching states is added to facilitate ZVS for the primary side's MOSFETs, and ZCS is obtained for the secondary side's power devices. It should be noted that C_t is designed to be significantly larger than the resonant capacitors and therefore it acts as a voltage source that has minor effect or none on the resonant behavior of the converter's phases. Further design details regarding the flying-capacitor are provided in Section III.

As can be observed from Fig. 2 and Fig. 3, the operation of the TIFLLC converter topology resembles a two-phase interleaved LLC converter with two input voltages for each phase that sum to V_{in}. As will be detailed in the next section, the voltages adapt their value based on the voltage gain per phase and as a result, high immunity is achieved to mismatches between the phases' resonant components. In addition, the use of a flying-capacitor naturally equalizes the current distribution the current between the phases, which in turn, enhances the power processing characteristics of the converter.

III. Analysis of Primary Characteristics for the TIFLLC Converter Topology

The flying-capacitor used in the TIFLLC converter introduces several interesting characteristics. The applied voltage on the switching nodes SW_a and SW_b is half of the input voltage which lowers the voltage stress on three out of the four primary side's MOSFETs by half. It also allows for lenient conditions to achieve ZVS on all the primary side's MOSFETs, since the voltage swing on these transistors during the commutation period is only half the input voltage. Moreover, the applied voltage on the resonant tank is also lowered by half and allows a design of a resonant network with lower impedance, i.e. lower inductance for the same switching frequency. Another very important property that will be detailed in the next section is the charge-balance on the flying-capacitor that provides current distribution between the converter's phases.

The voltage of the flying-capacitor v_{Ct} is assumed constant V_{Ct} for a duration of a switching cycle due to its low voltage ripple. The flying-capacitor's voltage ripple Δv_{Ct} depends primarily on the load current and it is designed to be small, i.e. no more than ±5% of the nominal value of V_{Ct} that typically equals $V_{in}/2$. This selection of a sufficiently high flying-capacitor value also guarantees that the tanks' resonant frequency is not affected by this capacitor. The expression for Δv_{Ct} is calculated by the charge being transferred in each state, and can be expressed as

$$\Delta v_{Ct} = \frac{I_{out}}{4nf_s C_t}, \tag{1}$$

where I_{out} is the load current, f_s is the switching frequency and n is the transformer's turns ratio.

The DC voltage of the flying-capacitor in the ideal case, i.e. the case of identical resonant components for both phases, equals $V_{in}/2$. For any other case, there may be a drift of V_{Ct} which is a result of the gain difference between the phases. Under first

TABLE I – Case Study Parameters Values

Component	*Value / Type*
Input voltage V_{in}	400 V
Output voltage V_o	12 V
Transformer's turns ratio n	8
Phase a resonant frequency f_r	~150 KHz
Phase a resonant capacitor C_{ra}	44 nF
Phase a resonant inductor L_{ra}	25 µH
Phase a magnetizing inductor L_{ma}	150 µH

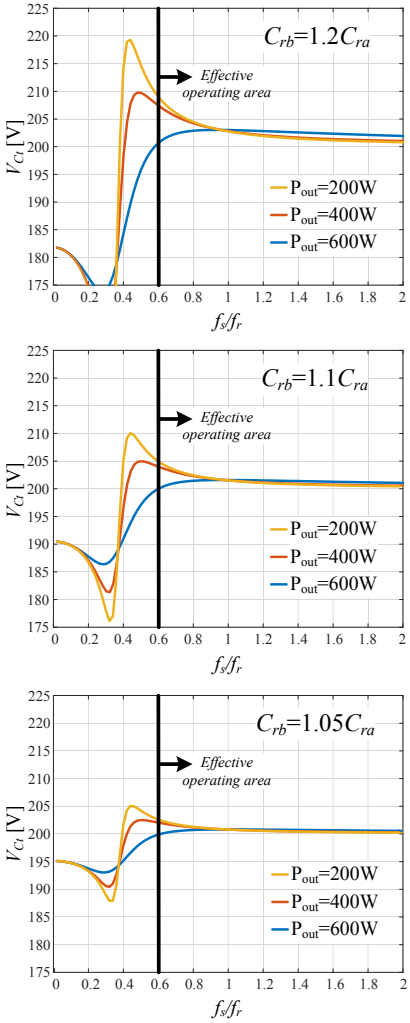

Fig. 4. Flying-capacitor voltage as a function of the switching frequency for phases with different resonant capacitors.

harmonic approximation (FHA) the normalized voltage gains G_a and G_b (for phases a and b, respectively) are expressed as:

$$G_a(f_s) = \frac{nV_{out,ac}}{V_{ina,ac}} = \frac{1}{\left(1+\frac{L_{ra}}{L_{ma}}-\frac{L_{ra}}{L_{ma}}\frac{1}{f_{na}^2}\right)+j\frac{\sqrt{L_{ra}/C_{ra}}}{n^2R_{ac,a}}\left(f_{na}-\frac{1}{f_{na}}\right)} \tag{2}$$

$$G_b(f_s) = \frac{nV_{out,ac}}{V_{inb,ac}} = \frac{1}{\left(1+\frac{L_{rb}}{L_{mb}}-\frac{L_{rb}}{L_{mb}}\frac{1}{f_{nb}^2}\right)+j\frac{\sqrt{L_{rb}/C_{rb}}}{n^2R_{ac,b}}\left(f_{nb}-\frac{1}{f_{nb}}\right)} \tag{3}$$

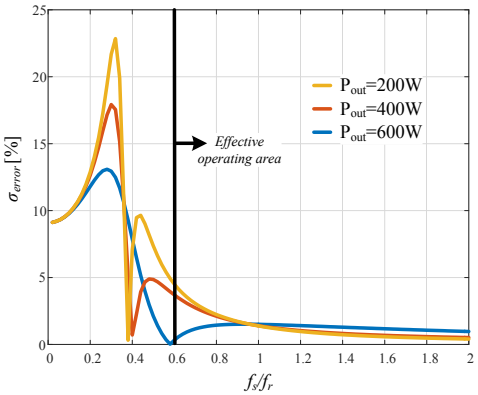

Fig. 5. Current error between the phases as a function of the switching frequency for C_{rb}=1.2C_{ra}.

where $V_{ina,ac}$ and $V_{inb,ac}$ are the ac input voltages of the phases *a* and *b*, respectively, given by:

$$V_{ina,ac}=\frac{V_{in}-V_{Ct}}{2},\quad V_{inb,ac}=\frac{V_{Ct}}{2}, \tag{4}$$

and f_{na}, f_{nb} are the normalized switching frequencies of phases *a* and *b*, defined as:

$$f_{na}=\frac{f_s}{f_{ra}}=\frac{f_s}{1/2\pi\sqrt{L_{ra}C_{ra}}},\quad f_{nb}=\frac{f_s}{f_{rb}}=\frac{f_s}{1/2\pi\sqrt{L_{rb}C_{rb}}}. \tag{5}$$

Using (2)-(4) and after some manipulations, the flying-capacitor voltage can be extracted and expressed as:

$$V_{Ct}\left(f_s\right)=\frac{V_{in}}{1+\frac{\left|G_b\left(f_s\right)\right|}{\left|G_a\left(f_s\right)\right|}}. \tag{6}$$

This implies that in case that the voltage gains of the phases are not equal, e.g. due to components' tolerances, the voltage deviates from the V_{in}/2 value and also depends on the switching frequency. Fig. 4 shows the variance in flying-capacitor voltage as a result of components' difference between the phases as a function of the normalized switching frequency, where in each case the resonant capacitor has been changed and the case study parameters are detailed in Table I. It can observed that for higher output power the voltage deviation from 200V is smaller compared to lower output power. It can also be observed that the overall deviation, even for the lower power case, is relatively small for the switching frequency's area of interest (marked with arrow on Fig. 4) where ZVS is achieved, i.e. above 0.6f_r.

IV. Current Sharing under Parameter Variations

Current sharing of multi-phase LLC converters has been widely investigated in [12]-[24]. In the TIFLLC converter topology, the charge-balance of the flying-capacitor assists in passive current sharing between the phases. Two MOSFETs conduct the current of the flying-capacitor: these are Q_{1a} during state I and Q_{1b} during state II, i.e.

$$i_{Ct}=\begin{cases} i_{Q1a} & @\,state\,I \\ -i_{Q1b} & @\,state\,II \end{cases}. \tag{7}$$

Since charge-balance on this capacitor exists, the average current through it must be zero, and the average currents through these two MOSFETs in every switching cycle are equal, i.e.

$$\left\langle i_{Q1a}\right\rangle=\left\langle i_{Q1b}\right\rangle. \tag{8}$$

Neglecting power loss in the system and assuming that the efficiency is high, the following holds

$$P_{in,a}=P_{out,a},\qquad P_{in,b}=P_{out,b}, \tag{9}$$

where P_{in} and P_{out} are the average input and output powers of each phase. The equality of (9) can be rewritten as

$$\begin{aligned} P_{in,a}&=\left\langle v_{in,a}\right\rangle\left\langle i_{in,a}\right\rangle=\frac{V_{in}-V_{Ct}}{2}\left\langle i_{Q1a}\right\rangle=I_{out,a}^2R_{ac,a}=V_{out}I_{out,a}\\ P_{in,b}&=\left\langle v_{in,b}\right\rangle\left\langle i_{in,b}\right\rangle=\frac{V_{Ct}}{2}\left\langle i_{Q1b}\right\rangle=I_{out,b}^2R_{ac,b}=V_{out}I_{out,b}\end{aligned}, \tag{10}$$

where $I_{out,a}$ and $I_{out,b}$ are the average output currents of the phases. From (8)-(10) it can be derived that the ratio between the two phases' output currents equals the ratio between the input voltages of the two phases, i.e.:

$$\frac{I_{out,a}}{I_{out,b}}=\frac{V_{in,a}}{V_{in,b}}=\frac{V_{in}-V_{Ct}}{V_{Ct}}. \tag{11}$$

The expression in (11) provides an insight to the current balancing mechanism that is achieved with using the flying-capacitor. The voltage V_{Ct}, as opposed to V_{in}, can dynamically change and as a result both $V_{in,a}$ and $V_{in,b}$ would vary accordingly. In the case that both the input and output voltages are common for the two phases, a mismatch of the resonant components results in voltage gains G_a and G_b that differ from the effective input-to-output ratio. The operation of the flying-capacitor automatically corrects the effective phase's input voltage (and as a result the input-to-output ratio) to comply with the variation in the voltage gain. The balancing action exceeds beyond the simplistic property of components variations for other parameters of the system such as the turn ratios of the phases' transformers.

Using the expression in (6) and after some manipulations, the ratio between the phases' output currents can be expressed as

$$\frac{I_{out,a}}{I_{out,b}}=\frac{G_b}{G_a}, \tag{12}$$

where G_a and G_b are the normalized voltage gains of the each phase. The current error between the two phases (the ratio between the difference and sum of the output currents, as defined in [19]), can be expressed as

$$\sigma_{error}=\left|\frac{G_a-G_b}{G_a+G_b}\right|. \tag{13}$$

Fig. 5 shows the value of (13) as a function of the switching frequency and the output power for a case of a converter with

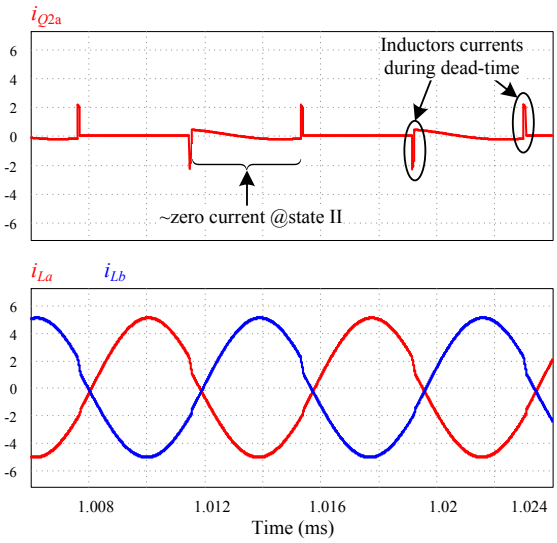

Fig. 6. Zero current characteristic of Q_{2a}.

TABLE II – EXPERIMENTAL PROTOTYPE'S PARAMETERS VALUES

Component	***Value / Type***
Input voltage V_{in}	400 V
Output voltage V_o	12 V
Flying capacitor C_t	3 µF
Output capacitance C_{out}	1 mF
Phase *a* transformer's turns ratio n_a	9
Phase *b* transformer's turns ratio n_b	9.3
Phase *a* resonant frequency f_{ra}	~138 KHz
Phase *b* resonant frequency f_{rb}	~130 KHz
Phase *a* resonant capacitor C_{ra}	66 nF ±10%
Phase *b* resonant capacitor C_{rb}	66 nF ±10%
Phase *a* resonant inductor L_{ra}	20 µH
Phase *b* resonant inductor L_{rb}	23 µH
Phase *a* magnetizing inductance L_{ma}	150 µH
Phase *a* magnetizing inductance L_{mb}	155 µH

parameters that are as given in Table I, and the variation in the resonant capacitor of phase *b* is by 20% compared to the resonant capacitor of phase *a*, i.e. C_{rb}=1.2C_{ra}. It can be observed that for a switching frequency higher than 0.6f_r the current error is less than 5% which is an attractive attribute for passive current sharing even at such an extreme case of components' difference.

The very good current distribution in the TIFLLC topology also contributes to enhanced power processing characteristics since the net current flowing through Q_{2a} is zero, as shown in Fig. 6.

V. EXPERIMENTAL RESULTS

To validate the operation of the TIFLLC converter operation, a 600W, 400V-to-12V prototype was built and tested. The transformers of both phases were hand made to create a difference between the resonant components of the phases and their measured leakage and magnetizing inductance are detailed in Table II. In addition, to further create a difference between the phases' parameters, the turn ratios of the transformers were designed to be not equal. The rest of components values and

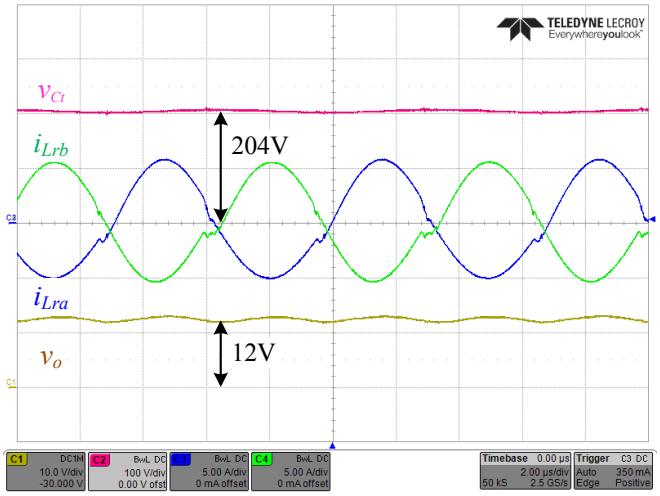

Fig. 7. Experimental waveforms of the TIFLLC converter. C1 – output voltage v_o (5V/div), C2 – flying-capacitor voltage v_{Ct} (100V/div), C3 – phase *a* primary-side resonant tank current i_{Lra} (5A/div), C4 – phase *b* primary-side resonant tank current i_{Lrb} (5A/div). Time scale is 2µs/div.

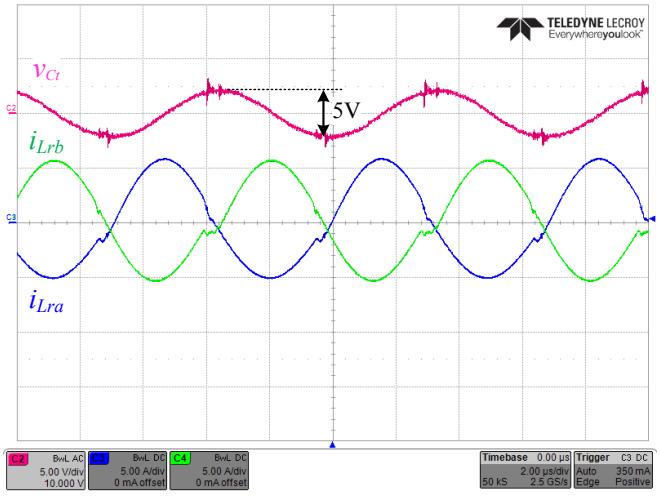

Fig. 8. Experimental waveforms of the TIFLLC converter. C2 – flying-capacitor voltage v_{Ct} (5V/div, ac coupled), C3 – phase *a* primary-side resonant tank current i_{Lra} (5A/div), C4 – phase *b* primary-side resonant tank current i_{Lrb} (5A/div). Time scale is 2µs/div.

parameters of the TIFLLC experimental prototype are given in Table II. The converter is digitally controlled using an FPGA using fully digital high performance ADC and DPWM peripherals as detailed in [26].

Figs. 7 to 9 show the converter's waveforms for output current of 50A (full load). Fig. 7 shows the flying-capacitor voltage, output voltage and the primary-side's currents of the two phases. As can be observed, in spite of the difference between the parameters of the phases, the phases' currents are almost equal with a very small difference between them, with a measured current error of 0.4%. In addition, the flying-capacitor voltage is 204V which is very close to V_{in}/2, as expected by the theoretical analysis from Section III. Depicted in Fig. 8 is the voltage ripple of the flying-capacitor Δv_{Ct} with a magnitude of around 5V, which is approximately 2.5% of V_{Ct}. Fig. 9Fig. 9

depicts the switching nodes SW_a and SW_b. As can be observed, ZVS of the primary-side's MOSFETs is obtained and the voltage of the switching nodes is around 200V (half of V_{in}) when they are high. Efficiency measurements of the converter for the two setups are provided in Fig. 10, demonstrating a peak efficiency of 97.3% and above 96% for most of the load range.

VI. Conclusion

A new two-phase interleaved flying capacitor LLC converter topology has been presented. The topology comprises two-phases for high current delivery and uses a flying capacitor to lower the voltage stress on the switches, balance the current distribution between the phases and enhance the power processing capabilities. The converter preserves all the benefits of conventional LLC converters while maintaining low sensitivity to resonant tank parameters mismatch and conventional driving circuitry with no extra components. Full principle of operation has been described, as well as the converter's primary characteristics and the impact of non-ideal components on the current sharing behavior. Preliminary results of the new converter show promising power processing characteristics, making the converter an attractive candidate as front-end converter for high output current applications.

References

[1] B. Yang, F. C. Lee, A. J. Zhang, and H. Guisong, "LLC resonant converter for front end DC/DC conversion," in *Proc. IEEE Appl. Power Electron. Conf. Expo. (APEC)*, Mar. 2002, pp. 1108-1112.

[2] B. Yang, Topology investigation for front end dc/dc power conversion for distributed power system, PhD Dissertation, Virginia Polytechnic Institute and State University, 2003.

[3] G. Ivensky, S. Bronshtein, and A. Abramovitz, "Approximate analysis of resonant LLC DC-DC converter", *IEEE Trans. Power Electron.*, vol. 26, pp. 3274-3284, Nov. 2011.

[4] I. Batarseh, "Resonant converter topologies with three and four energy storage elements," *IEEE Trans. Power Electron.*, vol. 9, pp. 64-73, Jan. 1994.

[5] R. P. Severns, "Topologies for three-element resonant converters," *IEEE Trans. Power Electron*., vol. 7, pp. 89-98, Jan. 1992.

[6] S. Luo, Z. Ye, R.-L. Lin, and F. C. Lee, "A classification and evaluation of paralleling methods for power supply modules," in *Proc. IEEE Power Electron. Spec. Conf. (PESC)*, vol. 2, Jul. 1999, p. 901-908.

[7] E. A. Burton, G. Schrom, F. Paillet, J. Douglas, W. J. Lambert, K. Radhakrishnan and M. J. Hill, "FIVR — Fully integrated voltage regulators on 4th generation Intel® Core™ SoCs," in *Proc. IEEE Appl. Power Electron. Conf. Expo. (APEC)*, 2014, Mar. 2014, pp. 432-439.

[8] G. Schrom, P. Hazucha, F. Paillet, D. J. Rennie, S. T. Moon, D. S. Gardner, T. Kamik, P. Sun, T. T. Nguyen, M. J. Hill, K. Radhakrishnan, and T. Memioglu, "A 100MHz eight-phase buck converter delivering 12A in 25mm2 using air-core inductors," in *Proc. IEEE Appl. Power Electron. Conf. Expo. (APEC)*, Mar. 2007, pp. 727–730.

[9] D. J. Perreault, R. L. Selders, and J. G. Kassakian, "Frequency-based current-sharing techniques for paralleled power converters," *IEEE Trans. Power Electron.,* vol. 13, no. 4, pp. 626–634, Jul. 1998.

[10] I. O. Lee, S. Y. Cho and G. W. Moon, "Interleaved buck converter having low switching losses and improved step-down conversion ratio," *IEEE Trans. Power Electron*., vol. 27, no. 8, pp. 3664-3675, Aug. 2012.

[11] T. Jin and K. Smedley: "Multiphase LLC series resonant converter for microprocessor voltage regulation", in *Proc. of IEEE 41st Industry Applications Conference – IAS,* vol. 5, Oct. 2006, pp. 2136 – 2143.

[12] E. Orietti, P. Mattavelli, G. Spiazzi, C. Adragna, and G. Gattavari, "Analysis of multi-phase LLC resonant converters," in *Power Electronics Conference, 2009. COBEP '09. Brazilian, 2009*, pp. 464-471.

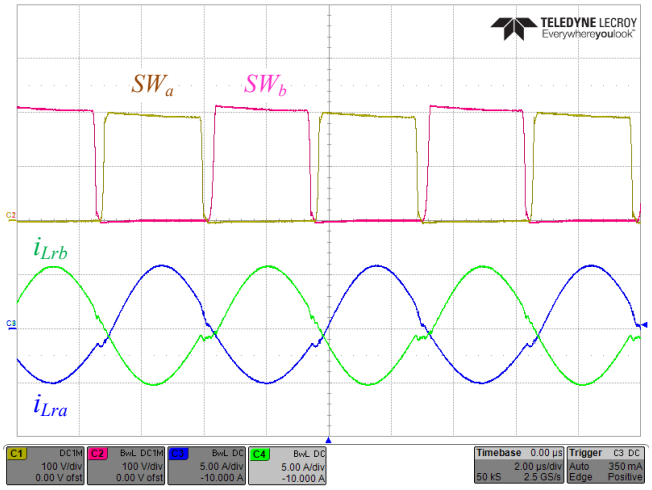

Fig. 9. Experimental waveforms of the TIFLLC converter. C1 – switching node voltage of phase *a* SW_a (100V/div), C2 – switching node voltage of phase *b* SW_b (100V/div), C3 – phase *a* primary-side resonant tank current i_{Lra} (5A/div), C4 – phase *b* primary-side resonant tank current i_{Lrb} (5A/div). Time scale is 2µs/div.

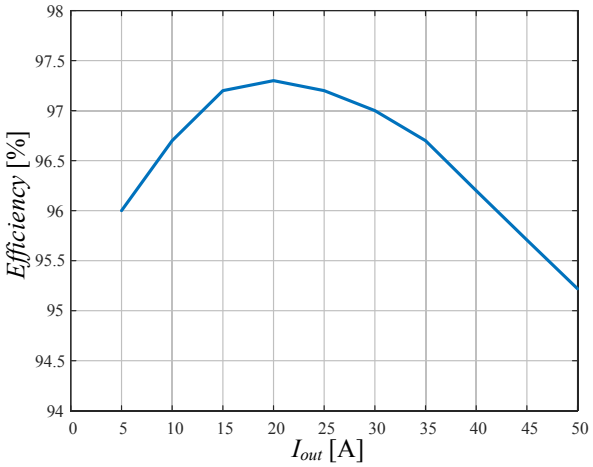

Fig. 10. Efficiency measurements of the experimental prototype.

[13] Z. Hu, Y. Qiu, L. Wang, and Y.-F. Liu, "An interleaved LLC resonant converter operating at constant switching frequency," *IEEE Trans. Power Electron*., vol. 29, pp. 2931-2943, Jun. 2014.

[14] Z. Hu, Y. Qiu, Y.-F. Liu, and P. C. Sen, "An interleaving and load sharing method for multiphase LLC converters," in *Proc. IEEE Appl. Power Electron. Conf. Expo. (APEC)*, Mar. 2013, pp. 1421-1428.

[15] E. Orietti, P. Mattavelli, G. Spiazzi, C. Adragna, and G. Gattavari, "Two-phase interleaved LLC resonant converter with current-controlled inductor," in *Power Electronics Conference, 2009. COBEP '09. Brazilian, 2009*, pp. 298-304.

[16] H. Figge, T. Grote, N. Froehleke. J. Boecker and P. Ide, "Paralleling of LLC resonant converter using frequency controlled current balancing", in *Proc. IEEE Power Electron. Spec. Conf. (PESC)*, Jun. 2008, pp. 1080 – 1085.

[17] E. Orietti, P. Mattavelli, G. Spiazzi, C. Adragna, and G. Gattavari, "Current sharing in three-phase LLC interleaved resonant converter, " in *Proc. IEEE Energy Convers. Conf. Expo. (ECCE)*, Sep. 2009, pp. 1145-1152.

[18] H. Wang, Y. Chen, Y. Qiu, P. Fang, Y. Zhang, L. Wang, Y.-F. Liu, and J. Afsharian, "A common capacitor multi-phase LLC converter with passive current sharing ability," *IEEE Trans. Power Electron.*, Early Access, 2017.

[19] H. Wang, Y. Chen, Y.-F. Liu, J. Afsharian and Z. Yang, "A Passive current sharing method with common inductor multi-phase LLC resonant converter," *IEEE Trans. Power Electron*., Early Access, 2017.

[20] H. Wang, Y. Chen, Y.-F. Liu, and S. Liu, "Automatic current-sharing method for multi-phase LLC resonant converter," *2016 IEEE 8th International Power Electronics and Motion Control Conference (IPEMC-ECCE Asia)*, Hefei, 2016, pp. 3198-3205.

[21] H. Wang, Y. Chen, and Y.-F. Liu, "A Passive-impedance-matching technology to achieve automatic current sharing for multi-phase resonant converter," *IEEE Trans. Power Electron.*, Early Access, 2017.

[22] B. C. Kim, K. B. Park, C. E. Kim, and G. W. Moon, "Load sharing characteristic of two-phase interleaved LLC resonant converter with parallel and series input structure, " in *Proc. IEEE Energy Convers. Conf. Expo. (ECCE)*, Sep. 2009, pp. 750-753.

[23] Y. Gang, P. Dubus, and D. Sadarnac, "Analysis of the load sharing characteristics of the series-parallel connected interleaved LLC resonant converter," in *2012 13th International Conference on Optimization of Electrical and Electronic Equipment (OPTIM),* May 2012, pp. 798-805.

[24] K. Bong-Chul, P. Ki-Bum, and M. Gun-Woo, "Analysis and design of two-phase interleaved LLC resonant converter considering load sharing," in *Proc. IEEE Energy Conversion Congr. Expo*. *(ECCE)*, Sep. 2009, pp. 1141-1144.

[25] F. Jin, F. Liu, X. Ruan and X. Meng, "Multi-phase multi-level LLC resonant converter with low voltage stress on the primary-side switches," in *Proc. IEEE Energy Convers. Conf. Expo. (ECCE)*, Sep. 2014, pp. 4704-4710.

[26] Y. Halihal, Y. Bezdenezhnykh, I. Ozana, M. M. Peretz, "Full FPGA-based design of a PWM/CPM controller with integrated high-resolution fast ADC and DPWM peripherals," IEEE Workshop on Control and Modeling for Power Electronics (COMPEL), Jun. 2014, pp. 1-5.